Cement & Concrete Composites 34 (2012) 62–67

Contents lists available at ScienceDirect

Cement & Concrete Composites

journal homepage: www.elsevier.com/locate/cemconcomp

Influence of fiber chemical coating on the acoustic emission behavior of steel fiber reinforced concrete

D.G. Aggelis *, D.V. Soulioti, N.M. Barkoula, A.S. Paipetis, T.E. Matikas

Department of Materials Science and Engineering, University of Ioannina, 45110 Ioannina, Greece

ARTICLE INFO

Article history:
Received 9 September 2010
Received in revised form 4 July 2011
Accepted 12 July 2011
Available online 22 July 2011

Keywords:
Four-point bending
Fracture mode
Frequency
Pull-out
Nondestructive monitoring

ABSTRACT

The current study focuses on the effect of chemical coating on the acoustic emission (AE) characteristics monitored during the fracture process in steel fiber reinforced concrete (SFRC). Different shapes of chemically treated and un-treated steel fibers are used to create specimens which are subjected to four point bending up to failure. Sensitive AE indices demonstrate that the coating gives distinct characteristics to the interface bonding between the fiber and the concrete matrix, which are evident mainly during the pull-out stage, after the moment of macroscopic crack formation. Specifically, AE average frequency and RA value, which defines the rising angle of the waveforms indicate that coating results in extensive matrix cracking in addition to the friction between fiber and concrete which characterizes the uncoated fibers. AE analysis can be used for interpretation of the fracturing stage and characterization of the fracture mode. It is shown that the surface conditioning of the fibers leaves a clear fingerprint on the AE signals, shedding light into the processes that occur during failure in SFRC.

1. Introduction

Concrete is characterized by some unique properties that make it the most common construction material worldwide such as its low cost, easiness of forming and high compressive strength. However, it exhibits low performance when subjected to tensile loads while its behavior is quite brittle. The traditional way to deal with the problem is the inclusion of reinforcement in the form of steel bars or more recently in the form of steel fibers. Although the compressive strength of fiber reinforced concrete is not reported to significantly increase, the material is characterized by higher tensile strength and significantly improved post-peak behavior and specifically toughness [1,2]. A fiber in the path of a propagating crack bridges the crack opening and resists further crack growth by dissipating energy during pull-out [3]. Different types of fibers have been used in concrete structures and pavements subjected to heavy dynamic loads. Fibers, contribute to improving concrete tensile and flexural strength, fatigue life, ductility, surface skin resistance to seawater wetting–drying cycles as well as to delaying concrete cracking due to alkali-aggregate reaction [4–8]. Fibers are also used in reinforcing concrete with corroding steel in order to maintain steel bond to concrete, and at the same time, reduce the resulting concrete cracking [9,10]. Straight steel fibers improve the bond between concrete and reinforcement in structural joints [11], while SFRC exhibits improved resistance to jet-induced spalling during vertical take-off of aircrafts [12] and improves the torsional behavior of concrete beams with or without conventional reinforcement [13].

However, the bonding between the fiber and the matrix may pose a severe limitation to the effective use of the fibers in high performance cementitious materials. Enhancing interface bond properties is especially important for high strength steel fibers which are commercially available as concrete reinforcement. The stress transfer efficiency, between these fibers and the matrix is a prerequisite to improve the properties of reinforced concrete [14], as well as to prevent premature debonding due to the internal stresses caused by the shrinkage of the matrix [15]. The major mechanisms that promote interfacial bond between concrete and steel are friction, mechanical anchorage and chemical adhesion induced by the application of fiber coating [11]. Different kinds of modifications have been attempted to improve the interfacial strength between reinforcement and matrix. Among those are chemical coating to instigate bonding [16] and mechanical processing (surface machining or surface sanding) of the reinforcing phase in order to achieve better contact between the constituent materials [17].

The fracture process in a material as complicated as SFRC includes different failure mechanisms, which concern plain concrete [18] (cracking, detachment of aggregates, aggregate crushing), the fibers, (plastic deformation and rupture), and the interface (debonding or friction) [3]. In addition, little is known of the chemical bond between the steel fibers and the cement matrix, as the stress transfer is mostly attributed to frictional shear stresses [15].

* Corresponding author. Tel.: +30 26510 08006; fax: +30 26510 08054.
E-mail address: daggelis@cc.uoi.gr (D.G. Aggelis).

0958-9465/$ - see front matter © 2011 Elsevier Ltd. All rights reserved.
doi:10.1016/j.cemconcomp.2011.07.003

In order to shed light to the complicated damage mechanics of this material, the acoustic emission technique has been used [19–22]. AE allows the passive observation of crack growth utilizing transducers placed on the surface of the material. These transducers record the transient response after any crack propagation incidence and convert it into an electric waveform [23], see Fig. 1. Each "cracking event" leads to elastic waves which are captured by the different sensors as "hits". Apart from the deterministic information that can be drawn about the location of the cracks and the cumulative activity, signal-based AE allows for more detailed fracture evaluations [24]. The features that have been extensively studied in relation to the fracture process are the average frequency, AF, which is the number of threshold crossings ("counts" in AE terminology, roughly equal to the wave oscillations) over the duration of each signal, measured in kHz, and the RA value which is the rise time over the maximum amplitude of the waveform, measured in μs/V (see Fig. 1). Rise time is the delay between the onset (first threshold crossing) and the highest peak of the waveform. The different types of failure processes, lead to wave emissions with distinct characteristics enabling the classification of cracks as to their mode [25,26]. Briefly, it can be stated that tensile mode of cracks, leads to emissions with higher frequency content as well as higher rise angle [27,28], as is schematically depicted in the bottom of Fig. 1. Shear types of failure such as delaminations, or fiber pull-out have been shown to produce signals with increased duration and lower frequency for concrete or other materials [27–30]. This is related to the elastic wave modes excited by the relative motion of the crack sides, which is different for each cracking mode [31] (motion perpendicular to the sides of the crack for mode I-tensile and parallel but opposite direction for mode II-shear), see again Fig. 1.

In the present study, SFRC beams are tested in four-point bending with concurrent monitoring of their AE activity. Three types of fibers were used, namely straight, with hooked ends and undulated (wavy), all with and without chemical coating in order to assess the effect of the chemical bonding on the acoustic emission (AE) characteristics. AE was monitored during the fracture process in steel fiber reinforced concrete for interpretation of the fracturing stage and fracture mode. This is, to the authors' knowledge the first reported study of AE on SFRC with chemically coated fibers. This study shows that detailed analysis of AE indices related to the acoustic waveform shape, provides much more sensitive information regarding the actual material failure process due to active damage mechanisms than quantitative parameters such as the cumulative AE activity. Although these damage mechanisms (friction, cracking) relate directly to the macroscopically measured mechanical properties, their interaction may mask the individual contribution of each distinct mechanism. However, the possibility to distinguish between them based on their acoustic imprint is a valuable tool towards the tailoring of the properties of the constituent phases for optimum performance.

2. Experimental details

Six different concrete mixtures were produced in total, with constant mixture proportions. The aggregates consisted of 25% coarse aggregates with maximum aggregate size 10 mm, and 75% crushed sand, while water/cement ratio was 0.50 by mass. The density and the water absorption of the sand were 2500 kg/m^3 and 2.44% respectively and of the coarse aggregate 2610 kg/m^3 and 1.05% respectively. The fiber content in concrete was 1% by volume, while three different shapes of the fibers were used, namely straight with aspect ratio (AR, length to diameter) 25 mm/0.4 mm = 63, undulated with AR = 30 mm/0.7 mm = 43 and fibers with hooked ends and AR again 30 mm/0.7 mm = 43. Specimens with coated and uncoated fibers were produced with a population of four specimens each. The chemical coating used to treat the surface of the fibers was a zinc phosphate (ZnPh) conversion coating introduced by Sugama et al. [16]. The formulation for the coating liquid was 0.46 wt.% zinc orthophosphate dihydrate, 0.91 wt.% 85% H_3PO_4, and 98.63 wt.% water [16].

The specimens were cured in water saturated with calcium hydroxide at 23 ± 2 °C for 28 days prior to testing. The specimens subjected to four-point bending were 100 × 100 × 400 mm in size with bottom and top spans 300 mm and 100 mm respectively (Fig. 2a). The displacement rate was 0.08 mm/min and the maximum mid span deflection was 2 mm according to ASTM C1609/C 1609 M-05. Details on the mechanical testing can be found in [6]. As to AE monitoring, two AE broadband sensors (Pico, PAC) were attached to the bottom tensile side of the specimen (Fig. 2b). Roller bearing grease was used for acoustic coupling, while the sensors were secured by the use of tape during the experiment. The signals were recorded in a two-channel monitoring board PCI-2, PAC with a sampling rate of 5 MHz, while in a previous study resonant sensors were used [29].

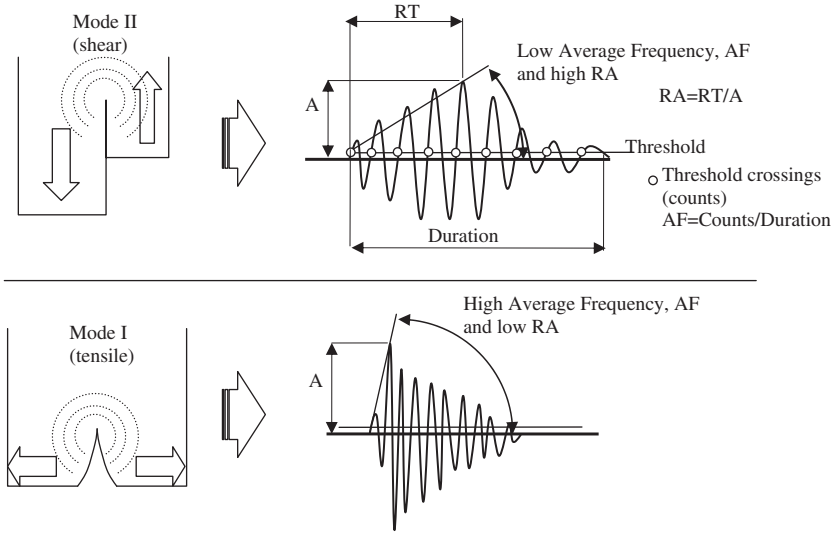

Fig. 1. AE sources and typical corresponding waveforms.

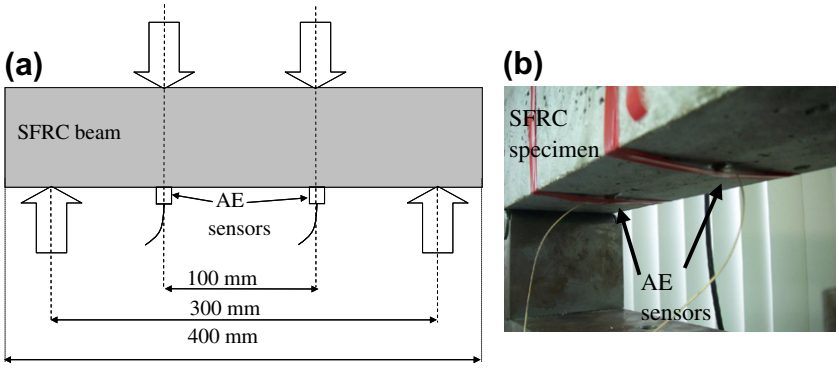

Fig. 2. (a) Representation of bending experiment. (b) Bottom surface of SFRC beam during bending with AE sensors attached.

3. Results

The cumulative AE behavior does not always exhibit distinct trends for the different types of specimens. Examples of the cumulative activity for four specimens are shown below along with their load–time history. Fig. 3a shows the cumulative activity for straight fibers and Fig. 3b for hooked fibers with and without coating. For all specimens, acquisition of AE starts shortly after load application. The AE hit line increases almost vertically at the moment of main fracture (marked by an arrow) which is followed by a clear drop of load for each case. Though not consistent for all the specimens tested, specimens with coated fibers exhibited increased AE activity. However, consistent differences are exhibited in qualitative parameters of AE presented below.

3.1. Straight fibers

Fig. 4a shows the average frequency, AF for the specimens presented in Fig. 3a. AF is presented as moving average of the recent 50 points in order to show the trend more clearly. AF starts at an average of approximately 400–500 kHz for both coated and uncoated specimens with some fluctuations. These hits are due to micro-cracking of the matrix since there is no evident macrocrack or any drop of load. At the moment of main fracture, there is a severe drop of the AF line (indicated by arrows), which for the case of uncoated fibers is more prominent (from 420 kHz to 100 kHz). After the main fracture event, the behavior is different for the two types of specimens, since for the coated, the AF increases gradually to the pre-peak levels of 400 kHz while the AF of the uncoated remains at lower levels, while both exhibit notable fluctuations.

Considerable differences are also observed for the RA value of specimens with straight coated and uncoated fibers (Fig. 4b). Initially for both coated and uncoated specimens RA lies below 500 μs/V. At the moment of fracture both lines exhibit sharp peaks which are the result of numerous hits with RA higher than the previous population. Thereafter the RA line of the uncoated follows a fluctuating but increasing trend up to 2000 μs/V, while the RA line of the coated remains at approximately 500 μs/V.

This behavior shows the transition from early matrix cracking to macro-cracking and pull-out, as will be discussed in a following section and it is consistent for all four specimens of each mixture. Another example of the same composition is shown in Figs. 4c and d concerning comparison of the AE indices between coated and uncoated straight fiber specimens. Again at the moment of fracture both specimens exhibit sharp drops in AF and peaks in RA value. After the main fracture incidence the uncoated clearly exhibits lower AF and higher RA lines until the end of the experiment.

3.2. Undulated and hooked fibers

Similar though not identical are the results obtained for specimens with undulated fibers. In this case, apart from the friction, mechanical interlocking is also active between fibers and matrix due to the geometry of the fibers. Fig. 5 shows the behavior of two specimens with undulated fibers as to their AF and RA. The basic trends remain the same with coated fiber specimens exhibiting higher frequency than the uncoated, especially after the main fracture. This shows that except pullout, matrix cracking is still active for coated specimens, which is confirmed by the lower RA that they exhibit. Fig. 6 shows the results for SFRC with hooked-end fibers. The trends are clearer than those obtained from the undulated fibers showing the distinct behavior of coated and uncoated fibers both in terms of AF and RA.

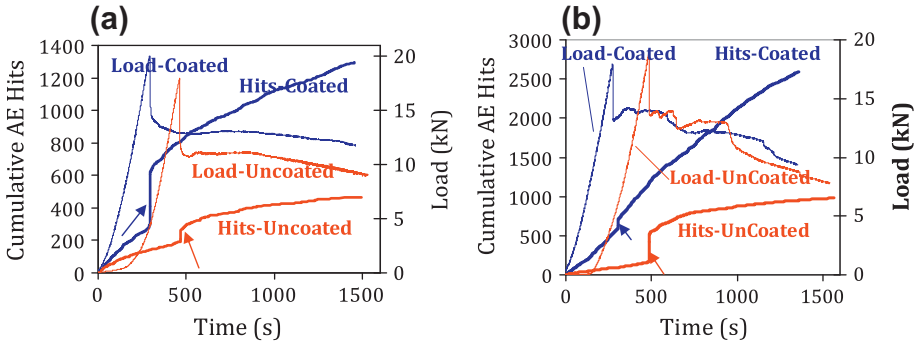

Fig. 3. Cumulative acoustic emission and load history for typical SFRC with (a) straight and (b) hooked fibers.

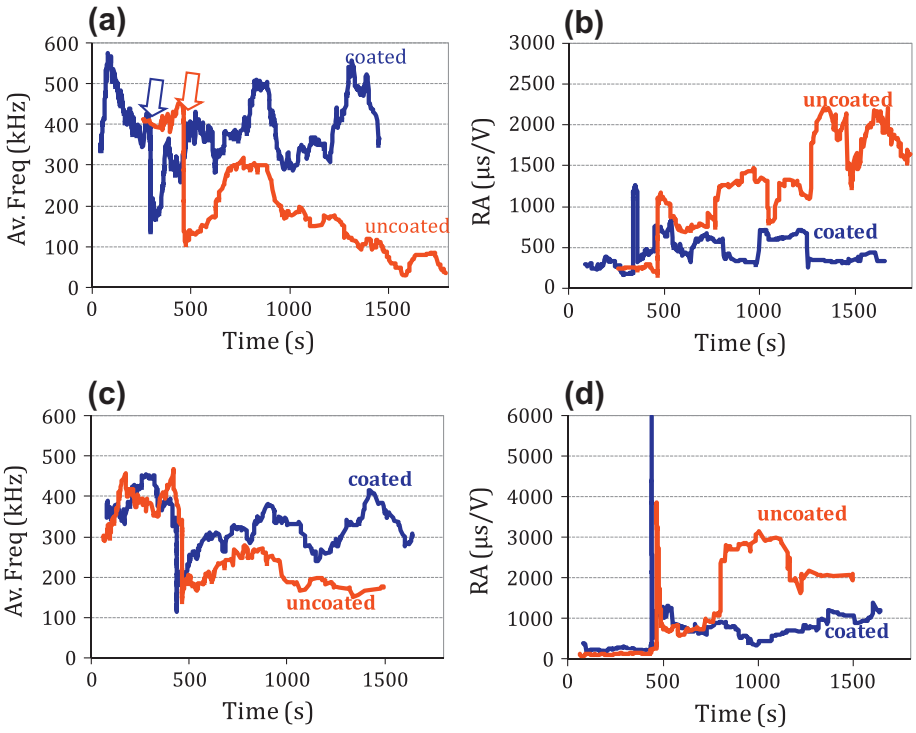

Fig. 4. (a and c) Average frequency, (b and d) RA history for typical SFRC specimens with straight fibers.

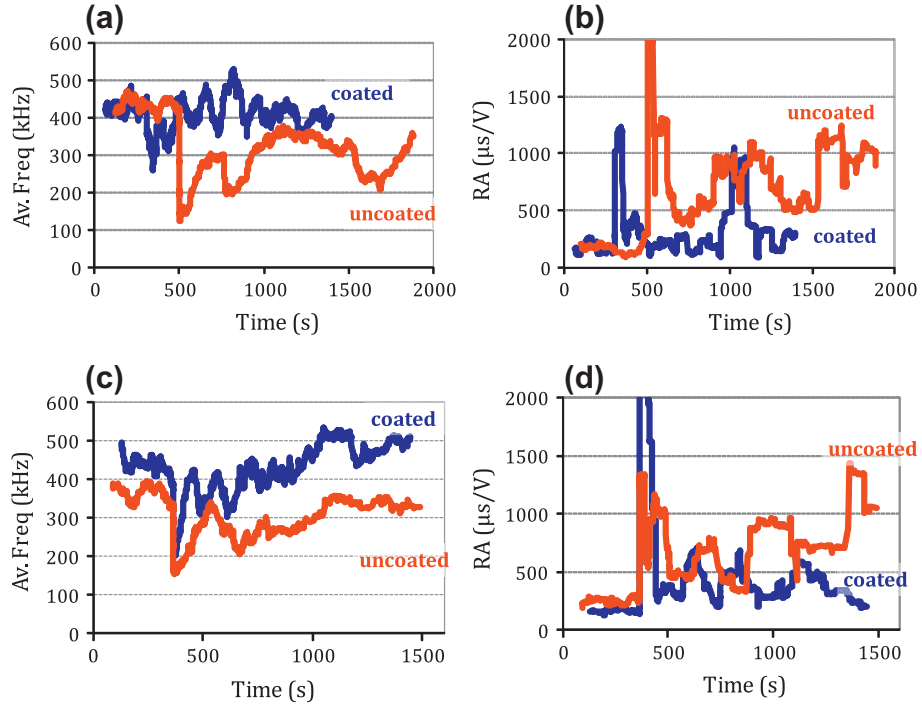

Fig. 5. (a and c) Average frequency (b and d) RA history for typical SFRC specimens with undulated fibers.

4. Discussion

It is interesting to discuss the above mentioned trends in respect to the corresponding fracture types. During the pre-peak stage AE activity can be attributed to matrix micro-cracking which is the only active mechanism. At the moment of main fracture, extensive matrix cracking and fiber pull-out occurs. After the main crack formation numerous pull-out events dominate the failure process. Since pull-out resembles fracture mode II it results in lower AF and higher RA than the matrix cracking stage. However, this behavior is much more evident for the uncoated specimens. In the case of uncoated fibers after primary fracture, the characteristics of AE activity imply mode II failure or pure friction between fibers and matrix. On the other hand, for the coated fibers, the higher

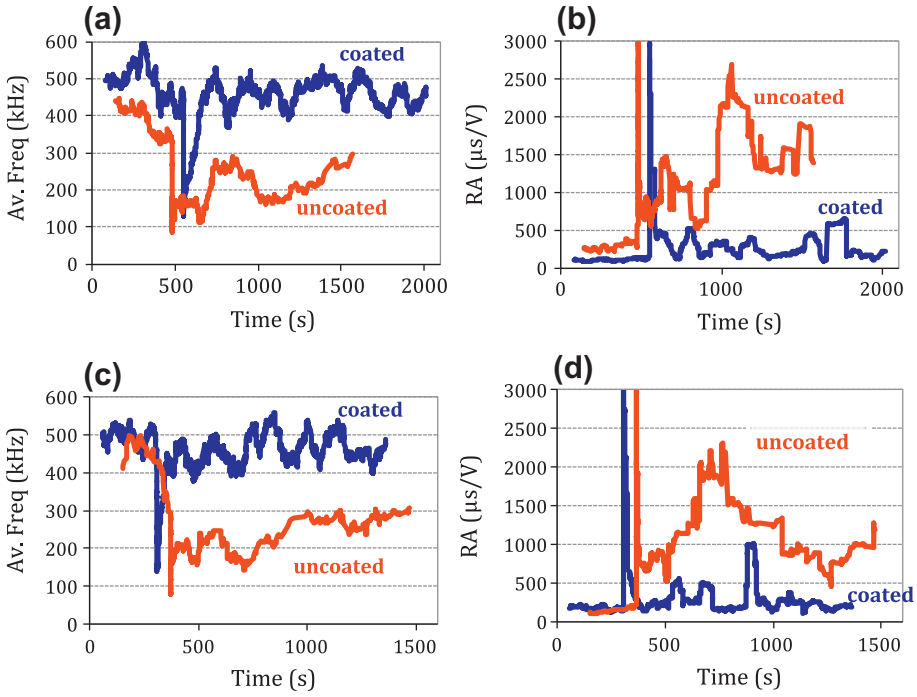

Fig. 6. (a and c) Average frequency (b and d) RA history for typical SFRC specimens with hooked fibers.

value of AF and lower RA imply that the coating is active and results in mode mixity, due to the better bond between fibers and concrete which deflects the crack propagation from the interface into the concrete matrix. In other words, when a coated fiber is loaded, clear interfacial failure leading to fiber pull-out is not the only possibility as cracks may propagate into the concrete matrix. This is the reason that AE characteristics show systematic differences between coated and uncoated fiber specimens, behavior which of course is more evident at the post-peak region where interfacial failure mechanisms at the fiber-concrete interface become active and contribute to the load redistribution.

Due to the complexity of the failure process in SFRC, the results are discussed in groups in relation to the fracture stage in order to examine their overall trend rather than focus on specific acoustic signals. The importance lies on the comparison between different types of materials and the study of the fracture processes occurring simultaneously with the AE trends. Fig. 7 depicts the AF as an average of all four specimens of each type of SFRC tested in bending for the different fracture stages (before, during and after main fracture). The first and global remark is the severe drop of frequency during the formation of the main crack. At the initial micro-cracking stage the frequency of the signals is, for any type of SFRC above 350 kHz, while the effect of coating is not consistent. During the macro-crack formation, which lasts for approximately 1 s and is accompanied by a number of more or less 100 AE hits, AF drops to less than 200 kHz. This trend is global for all mixtures, resulting from the contribution of pull-out from this moment on and shows the ability of AE to capture details related to the actual fracture process. This shows that by monitoring AE activity of a structure it is possible to characterize the fracture stage, based on specific AE indices that are measured nondestructively. Furthermore, what is of great significance for this study is that after the main fracture, the uncoated fiber specimens exhibit clearly lower AF than the coated ones. The difference is more prominent for the straight fibers were AF of the uncoated fiber specimens is less than 50% of the coated (151 kHz compared to 347 kHz). Equally evident is the difference for the hooked fibers specimens (258 kHz compared to 450 kHz), while the wavy fibers exhibit the lowest difference (311 kHz and 400 kHz for uncoated and coated respectively).

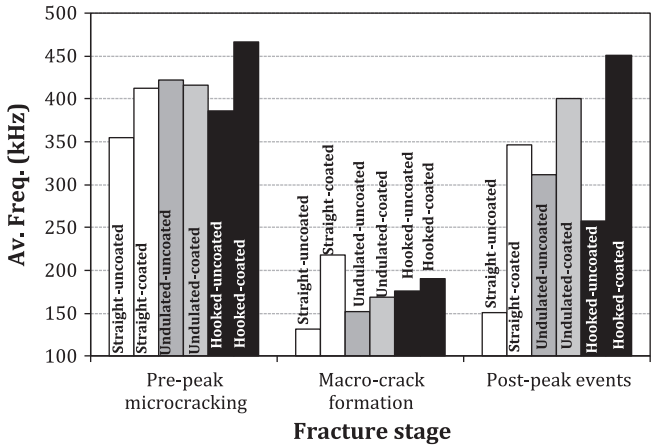

Fig. 7. Average frequency of SFRC with different fibers and surface conditioning.

Fig. 8 shows the corresponding trend of the RA value. Initially all different mixtures exhibit relatively low values. At the moment of main fracture RA rises by 10 or even 20 times, a trend reasonably explained by the severe processes including fiber pull-out which are developing at that time. Later there is a distinct difference concerning the chemical coating, with the uncoated fibers exhibiting higher values than coated. Again the straight fibers exhibit the largest discrepancy in RA at the pull-out stage (2054 μs/V for uncoated and 611 μs/V for coated), while the undulated exhibit the smallest discrepancy (719 μs/V for uncoated and 541 μs/V for coated). This is consistent with the results of AF, showing that the shape characteristics of the fibers, exercise similar influence on the different AE parameters during fracture. Additionally it is also reasonable that chemical coating is more important for straight fibers since their shape does not allow any mechanical

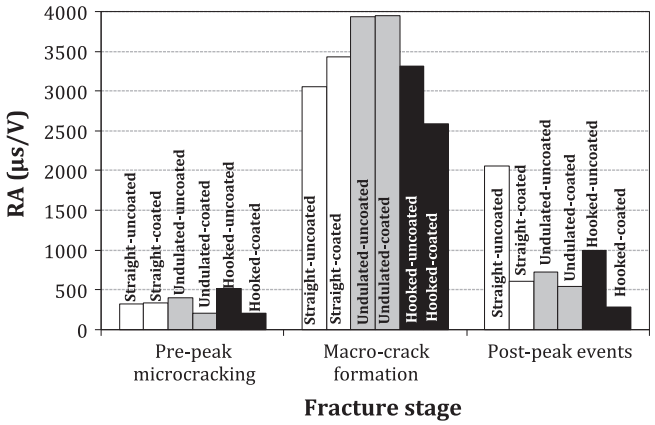

Fig. 8. RA of SFRC with different fibers and surface conditioning.

interlocking. Therefore, the difference due to the chemical bonding is much more evident. On the other hand, hooked or wavy fibers exhibit mechanical interlocking which anyway results in extensive matrix cracking during pull-out. For these fiber shapes, apart from the friction, which is apparently influenced by the coating, the matrix material near the vicinity of each fiber during their pull-out is cracked, leading to more "mixed-mode" signals, indicated by lower RA values and higher AF.

5. Conclusions

This paper presents the results of acoustic emission monitoring of steel fiber reinforced concrete with and without chemical coating on fibers of different shapes. The results reveal that the damage mechanisms exhibit distinct changes related to the shape of the fibers and the existence of the coating, resulting in clearly detectable changes in the acoustic behavior. The AE behavior is studied mainly by the use of average frequency and RA value which are correlated with damage mode. Low frequency and high RA demonstrate clearer friction characteristics for the case of uncoated fibers. On the other hand, specimens with chemically coated fibers, exhibit inverse trends concerning these AE characteristics, revealing that friction is not the only process in this case, but it is accompanied by matrix cracking due to the good bonding between fiber and matrix. The geometry of the fibers is also important since the straight fibers exhibit the purest shear characteristics implying that only friction forces are active during the pull-out stage, while hooked and wavy fibers contribute to matrix cracking during this stage. In general, for all different mixtures, AE provides the means to identify between different fracture stages, i.e. pre-peak and post-peak which is of great significance for monitoring of actual structures. These results indicate that detailed study of the AE behavior may provide insight to the macroscopical mechanical behavior, while other scanning techniques like SEM could further confirm the difference of the failure surface of different types of specimens.

Acknowledgement

The fibers were supplied by CHIRCU PROD-IMPEX COMPANY SRL, Romania.

References

[1] Stahli P, van Mier JGM. Manufacturing, fibre anisotropy and fracture of hybrid fibre concrete. Eng Fract Mech 2007;74:223–42.
[2] Chunxiang Q, Patnaikuni I. Properties of high-strength steel fiber-reinforced concrete beams in bending. Cem Concr Compos 1999;21:73–81.
[3] Pompo A, Stupak PR, Nicolais L, Marchese B. Analysis of steel fibre pull-out from a cement matrix using video photography. Cem Concr Compos 1996;18:3–8.
[4] Shah SP. Do fiber increase the tensile strength of cement-based matrixes. ACI Mater J 1991;88(6):595–602.
[5] Chenkui H, Guofan Z. Properties of steel fibre reinforced concrete containing larger coarse aggregate. Cem Concr Compos 1995;17:199–206.
[6] Soulioti DV, Barkoula NM, Paipetis A, Matikas TE. Effects of fibre geometry and volume fraction on the flexural behaviour of steel-fibre reinforced concrete. Strain 2011;47:e535–e41.
[7] Al-Tayyib AJ, Al-Zahrani M. Use of polypropylene fibres to enhance deterioration resistance of concrete sulfate skin subjected to cyclic wet/dry sea exposure. ACI Mater J 1995;89(4):363–70.
[8] Haddad R, Smadi M. Role of fibres in controlling unrestrained expansion and arresting cracking in Portland cement concrete undergoing alkali-silica reaction. Cem Concr Res 2004;34(1):103108.
[9] Haddad RH, Ashteyate AM. Role of synthetic fibres in delaying steel corrosion cracks and improving bond with concrete. Can J Civil Eng 2001;28:787–93.
[10] Almusallam AA, Al-Ghtani AS, Aziz AR, Rasheeduzzafar. Effect of reinforcement corrosion on bond strength. Constr Build Mater 1996;10(2):123–9.
[11] Haddad RH, Abendeh RM. Effect of thermal cycling on bond between reinforcement and fiber reinforced concrete. Cem Concr Compos 2004;26:743–52.
[12] Robins PJ, Austin SA. The resistance of steel fibre concrete to VTOL engine jet blast. Cem Concr Compos 1994;16:57–64.
[13] Chalioris CE, Karayannis CG. Effectiveness of the use of steel fibres on the torsional behavior of flanged concrete beams. Cem Concr Compos 2009;31:331–41.
[14] Wu HC, Li VC. Fiber/cement interface tailoring with plasma treatment. Cem Concr Compos 1999;21:205–12.
[15] Frantzis P, Baggott R. Bond between reinforcing steel fibres and magnesium phosphate/calcium aluminate binders. Cem Concr Compos 2000;22:187–92.
[16] Sugama T, Carciello N, Kukacka LE. Interface between zinc phosphate-deposited steel fibres and cement paste. J Mater Sci 1992;27:2863–72.
[17] Al-mahmoud F, Castel A, Francois R, Tourneur C. Effect of surface pre-conditioning on bond of carbon fibre reinforced polymer rods to concrete. Cem Concr Compos 2007;29:677–89.
[18] Kumar A, Gupta AP. Acoustic emission in fibre reinforced concrete. Exp Mech 1996;36(3):258–61.
[19] Aggelis DG, Shiotani T, Momoki S, Hirama A. Acoustic emission and ultrasound for damage characterization of concrete elements. ACI Mater J 2009;106(6):509–14.
[20] Wu K, Chen B, Yao W. Study on the AE characteristics of fracture process of mortar, concrete and steel–fiber-reinforced concrete beams. Cem Concr Res 2000;30:1495–500.
[21] Chen B, Liu J. Damage in carbon fiber-reinforced concrete, monitored by both electrical resistance measurement and acoustic emission analysis. Constr Build Mater 2008;22:2196–201.
[22] Weiler B, Grosse C. Pullout behavior of fibers in steel fiber reinforced concrete. Otto-Graf J 1996:116–27. <(http://www.mpa.uni- stuttgart.de/publikationen/otto_graf_journal/ogj_1996/beitrag_weiler.pdf)>.
[23] Grosse CU, Ohtsu M. Acoustic emission testing. Heidelberg: Springer; 2008.
[24] Grosse CU, Finck F. Quantitative evaluation of fracture processes in concrete using signal-based acoustic emission techniques. Cem Concr Compos 2006;28:330–6.
[25] Farid Uddin AKM, Numata K, Shimasaki J, Shigeishi M, Ohtsu M. Mechanisms of crack propagation due to corrosion of reinforcement in concrete by AE-SiGMA and BEM. Constr Build Mater 2004;18:181–8.
[26] Shiotani T. Evaluation of long-term stability for rock slope by means of acoustic emission technique. NDT&E Int 2006;39(3):217–28.
[27] Philippidis TP, Nikolaidis VN, Anastassopoulos AA. Damage characterization of carbon/carbon laminates using neural network techniques on AE signals. NDT&E Int 1998;31(5):329–40.
[28] Ohno K, Ohtsu M. Crack classification in concrete based on acoustic emission. Constr Build Mater 2010;24(12):2339–46.
[29] Soulioti D, Barkoula NM, Paipetis A, Matikas TE, Shiotani T, Aggelis DG. Acoustic emission behavior of steel fibre reinforced concrete under bending. Constr Build Mater 2009;23:3532–6.
[30] Aggelis DG, Barkoula NM, Matikas TE, Paipetis AS. Acoustic emission monitoring of degradation of cross ply laminates. J Acoust Soc Am 2010;127(6):EL246–51.
[31] Aggelis DG, Matikas TE, Shiotani T. Advanced acoustic techniques for health monitoring of concrete structures. In: Kim SH, Ann KY, editors. The Song's handbook of concrete durability. Middleton Publishing Inc.; 2010. p. 331–78.